Journal of Alloys and Compounds 488 (2009) 5–8

Contents lists available at ScienceDirect

Journal of Alloys and Compounds

journal homepage: www.elsevier.com/locate/jallcom

Magnetic and transport properties of Fe-rich thin cold-drawn amorphous wires

C. García[a], V. Zhukova[b], J. Gonzazez[a], A. Chizhik[a], J.M. Blanco[b], M. Ipatov[a], A. Zhukov[a,*]

[a] Dpto. Física de Materiales, Fac. Quimicas, Universidad del Pais Vasco, 20009 San Sebastian, Spain
[b] Dpto. Física Aplicada I, EUPSD, UPV/EHU, Plaza Europa 1, San Sebastián 20018, Spain

ARTICLE INFO

Article history:
Received 26 August 2007
Received in revised form 13 May 2008
Accepted 22 May 2008
Available online 23 January 2009

PACS:
75.50 Kj
75.80+q

Keywords:
Thin wires
Magnetic softness
Devitrification

ABSTRACT

Electrical resistivity, magnetic (saturation magnetization and switching field of the magnetic bistability) and magnetoimpedance measurements are reported in cold-drawn amorphous $Fe_{77.5}B_{15}Si_{7.5}$ thin wires of 14 μm diameter. Such measurements have been performed in the thin wire treated by current annealing. Electrical resistivity dependence with the intensity of the current flowing along the thin wire shows a deep decrease around 70 mA ascribed to the crystallization process. Dependence curve of the magnetization with the intensity of the current presents a change of slope at 40 mA which is ascribed to the nucleation of grains. Unusual dependence of switching field on applied stress exhibits a decrease of the switching field with the external stress in the as-prepared cold-drawn and post-treated thin wire. Magnetoimpedance ratio evolves from one to two peaks response increasing the frequency. Observed dependences interpreted taking into account strong internal stresses induced by the cold-drawn process.

1. Introduction

Nowadays, recent tendency in the miniaturization of devices to be used in different strategic industrial sectors (i.e., electronics, telecommunications, computers with more and more capacity of memory and speed of read and write,...) has produced a spectacular progress in the science and engineering of materials. In fact, advanced materials displaying fascinating magnetic properties with extremely low dimensions are of great interest for technological applications. Consequently, materials of different kinds satisfying those requirements have been developed and thoroughly investigated in the last recent years. In this context, wire-shaped materials with very small diameter that additionally exhibit excellent magnetic behaviour can be considered as a very promising candidates to cover such applications, paying special attention to the possibility for reducing the diameter from some hundreds microns (thin wires) down to a few nanometers (nanowires). Several technical approaches have been proposed for the preparation and processing of magnetic wires, such as non-equilibrium, rapid quenching, electroplating, or lithographic technologies [1–4].

On the other hand, soft magnetic amorphous and nanocrystalline alloys have attracted a great interest because such materials are very adequate materials to investigate fundamental aspects concerning the mechanisms governing their macroscopic magnetic properties. Among them thin wires with reduced geometrical dimensions (20 μm in diameter) could present special importance regarding industrial applications. With respect to their magnetic behaviour the bistability is one of the most interesting phenomena observed mainly in amorphous wires. This phenomenon is related with the single and large Barkhausen jump observed at certain conditions (for an applied magnetic field so-called "switching field", H_{sw}), between two remanent states [5,6]. Other important effect discovered in amorphous wires in 1994 [7,8] is the giant magnetoimpedance effect (GMI). This GMI effect is largest in amorphous wires with vanishing magnetostriction constant (up to 300–600% of change in the GMI ratio) and consists of magnetic field dependence of the electrical impedance Z of an amorphous and nanocrystalline ferromagnetic material (ribbon or wire). Such dependence is mainly determined by the magnetic domain structure and also related with the microstructure, elastic properties, magnetostriction and atomic mobility which allow magnetic anisotropy to be induced in some specially chosen alloys [9,10].

In this work we present a study on magnetic and transport properties of the cold-drawn amorphous $Fe_{77.5}B_{15}Si_{7.5}$ thin wire with 14 μm of diameter, which can be considered as an extension of a previous work [11], where a similar study was reported for the cold-drawn thin wire of 50 μm with the same composition.

2. Experimental details

Amorphous $Fe_{77.5}B_{15}Si_{7.5}$ thin wires of 125 μm diameter were obtained by the in-rotating water technique (rapid solidification) and after a post-processing of cold-drawn its diameter was reduced down to 14 μm. Pieces of 10 cm in length of the

* Corresponding author. Tel.: +34 943 018 611; fax: +34 943 017 130.
E-mail address: arkadi.joukov@ehu.es (A. Zhukov).

0925-8388/$ – see front matter © 2009 Published by Elsevier B.V.
doi:10.1016/j.jallcom.2008.05.111

14 μm diameter wire were cut to perform electrical resistivity, magnetic and magnetoimpedance measurements. The samples were submitted to thermal treatments by means of the current annealing technique (intensity ranging 0–80 mA) [12,13]. Structural information has been obtained from the thermal dependence of the electrical resistance using the four points method and magnetization versus temperature measurements (the increase of the temperature inside sample is obtained by flowing the electrical current). Hysteresis loops of the thin wires were obtained by a conventional induction method. Giant magnetoimpedance effect, GMI, at frequencies up to 500 MHz has been measured in both as-prepared state and after annealing.

3. Experimental results and discussion

3.1. Electrical resistivity and magnetization versus intensity of the electric current

The evolution of the electrical resistivity (ρ) with the electrical current intensity (I) flowing along the thin wire is presented in Fig. 1. The electrical current produces an increase of the temperature, T_X, inside the thin wire, so this figure could be equivalent to $\rho(T)$. As can be seen, ρ increases with I of a consequence of a large disorder connected to the structural relaxation. Around 70 mA there is a significant decrease associated to the crystallization as has been widely reported for the amorphous alloys [14].

Fig. 2 shows the variation of the saturation magnetization with the electrical current intensity. As it has been mentioned, it could be equivalent to the thermal dependence of the saturation magnetization. There is a change of tendency around 40 mA which could be ascribed to the beginning of the crystallization (nucleation process), appearing two phases (*bcc*-Fe(Si) crystalline and remaining amorphous matrix) in the thin wire after thermal treatment above 40 mA.

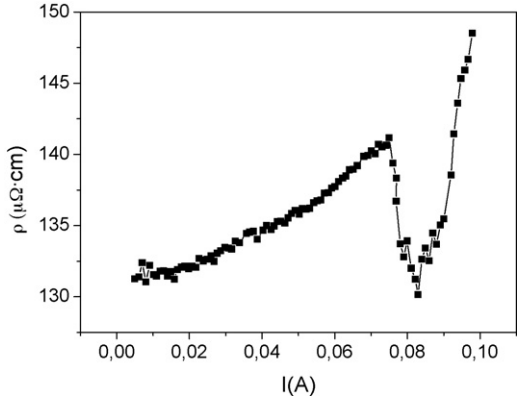

Fig. 1. Variation of the electrical resistivity with the intensity of the electric current flowing along the $Fe_{77.5}B_{15}Si_{7.5}$ cold-drawn thin wire of 14 μm of diameter.

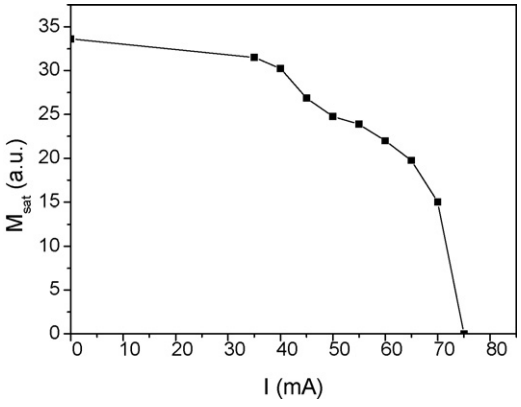

Fig. 2. Saturation magnetization versus intensity of the electric current flowing along the $Fe_{77.5}B_{15}Si_{7.5}$ cold-drawn thin wire of 14 μm of diameter.

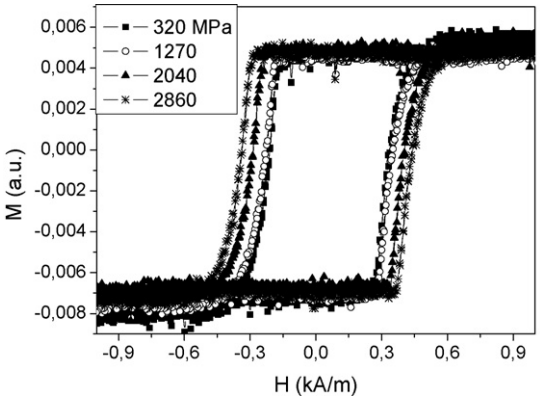

Fig. 3. Hysteresis loops of $Fe_{77.5}B_{15}Si_{7.5}$ cold-drawn thin wire of 14 μm of diameter under the action of applied tensile stress.

3.2. Magnetic bistability

Hysteresis loops of the cold-drawn thin wire under the effect of a tensile stress (σ) are shown in Fig. 3, which a rectangular shape typically of the bistable character. From these hysteresis loops the switching field, H_{SW}, has been evaluated as a function of the applied tensile stress, σ (Fig. 4). H_{SW} decreases monotonously as increasing σ in similar way to that found in cold-drawn thin wire of 50 μm [11], although the values of H_{SW} are larger in the thin wire of 14 μm in diameter. In the case of the thin wire of 125 μm, $H_{SW}(\sigma)$ decreases at low σ values to finally achieve a minimum value and then increases following a $\lambda^{1/2}$ law [15,16], which allows to assign a nucleation wall mechanism at the ends of the thin wires. Such decrease of $H_{SW}(\sigma)$ results from the competition between the applied tensile stress and the complex internal stresses with a significant component of compressive character and the maximum applied stress in the thin wire of 14 μm cannot overlap the internal stresses as occurs in the thin wire of 125 μm. In addition, the tensile stress that produce the break of the thin wire increases as the diameter decreases (according to the results of the thin wire of 20, 50 and 125 μm).

Fig. 5 presents the switching field of the bistable behaviour as a function of the mechanical tensile stress, σ, of the cold-drawn thin wire submitted to current annealing of 40 mA at different annealing times. Similarly, H_{SW} decreases monotonously with σ in all treated samples towards the same minimum value (around 45 MPa). The observed decrease of the switching field when the thermal treatment increases is related with the relaxation of the frozen internal stresses with temperature.

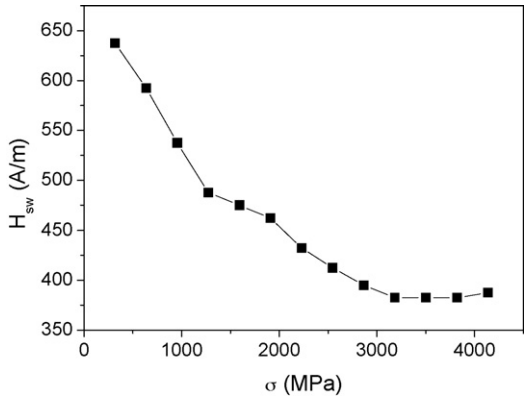

Fig. 4. Variation curve of the switching field with the applied tensile stress of $Fe_{77.5}B_{15}Si_{7.5}$ cold-drawn thin wire of 14 μm of diameter.

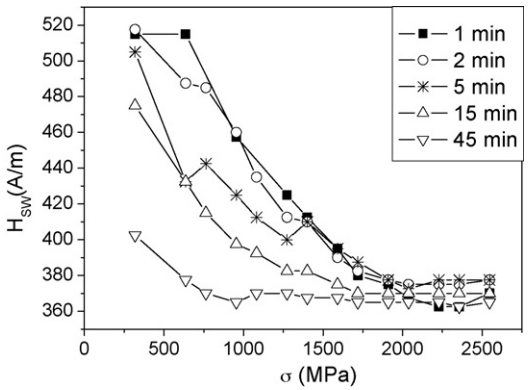

Fig. 5. Variation curves of the switching field with the applied tensile stress of $Fe_{77.5}B_{15}Si_{7.5}$ cold-drawn thin wire of 14 μm of diameter treated at 40 mA with different annealing time.

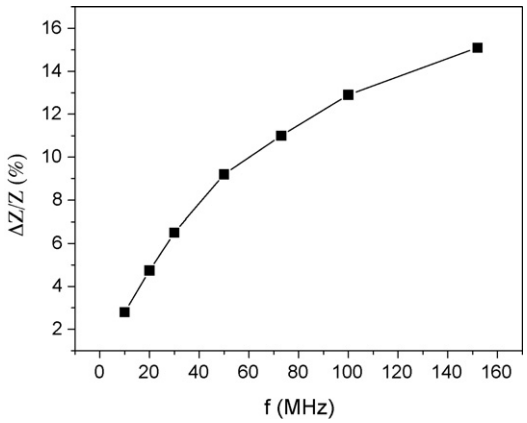

Fig. 7. Variation of the maximum GMI ratio reaches in each frequency of the cold-drawn thin wire.

3.3. GMI Effect

The GMI ratio as a function of the applied magnetic field for different frequencies of the cold-drawn thin wire is presented in Fig. 6(a–d). To note the hysteretic dependence observed at all frequencies. There is an increase of the GMI ratio with the frequency. Additionally, the character of GMI curves changes increasing the frequency from a single peak curves (at frequency approximately below 30 MHz) to double peaks at high frequency (above 100 MHz), which can be ascribed to the circumferential magnetic anisotropy of the surface layer. This behaviour is quite similar to that found in the thin wire with 50 μm of diameter. The variation of the maximum GMI ratio reaches in each frequency is presented in Fig. 7, which reflects the inhomogeneity (increasing) of the circumferential anisotropy across the radius.

In Fig. 8, the magnetic field dependence of impedance of stress annealed sample measured at 10 MHz is shown. As can be noted from the comparison of Figs. 8 and 6 increasing of the GMI ratio and the field of maximum take place. The observed changes can be attributed to the induction of the transversal magnetic anisotropy due to the stress annealing.

Concluding, dependence of the electrical resistivity and saturation magnetization with the intensity of the current flowing along the thin wire provide useful information on the crystallization of $Fe_{77.5}B_{15}Si_{7.5}$ cold-drawn thin wire of 14 μm. The stress dependence of the switching field is different to that reported in

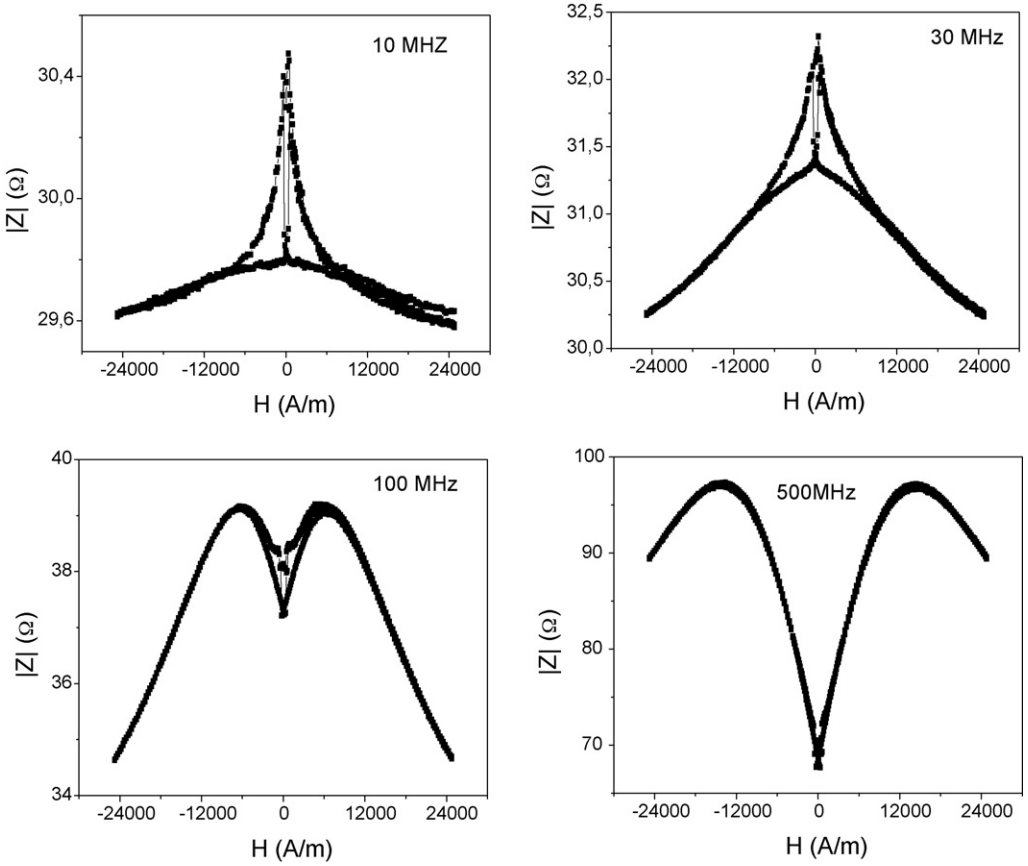

Fig. 6. GMI ratio as a function of the applied magnetic field for different frequencies of the cold-drawn thin wire: (a) 10 MHz; (b) 30 MHz; (c) 100 MHz and (d) 500 MHz.

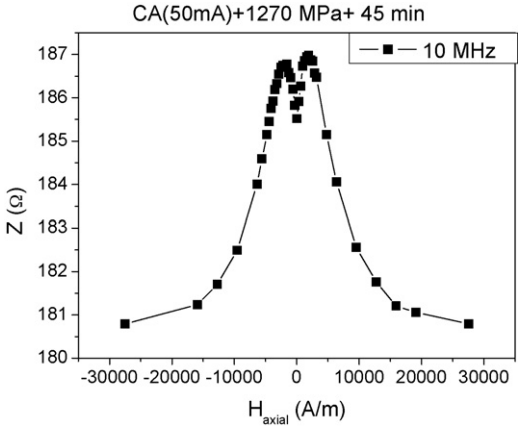

Fig. 8. GMI ratio as a function of the applied magnetic field for 10 MHz of the cold-drawn thin wire treated by stress annealing.

the initial thin wire with 125 μm in diameter. Significant GMI, $\Delta Z/Z$ effect (10–500 MHz) is observed. Hysteretic dependences of $\Delta Z/Z$ on applied axial magnetic field, H, in as-prepared state are attributed to the strong internal stresses. Such hysteretic behaviour of $\Delta Z/Z(H)$ disappears after current annealing.

References

[1] C.A. Ross, Annu. Rev. Mater. Res. 31 (2002) 203.
[2] L. Scott, in: H.S. Nalwa (Ed.), Magnetic Nanostructures, American Scientific Publishers, 2002 (Chapter 11).
[3] J. Gonzalez, A. Zhukov, Amorphous and nanocrystalline soft magnetic materials, in: Y. Liu, D.J. Sellmyer, D. Shindo (Eds.), Advanced Magnetic Materials, Book III Processing of Advanced Magnetic Materials, vol. 3, Kluwer Academic Publishers, Norwell, MA, USA, 2004, Chapter 5, pp. 115–181. (ISBN: 1-4020-7983-4)).
[4] F.B. Humphrey, J. Magn. Magn. Mater. 249 (2002) 1.
[5] F.B. Humphrey, K. Mohri, J. Yamasaki, H. Kawamura, R. Malmhall, I. Ogasawara, in: A. Hernando, V. Madurga, M.C. Sánchez-Trujillo, M. Vázquez (Eds.), Magnetic Properties of Amorphous Metals, Elsevier Scientific Publ., 1987, p. 110.
[6] J. González, J. Appl. Phys. 79 (1996) 376.
[7] L.V. Panina, K. Mohri, Appl. Phys. Lett. 65 (1994) 1189.
[8] R.S. Beach, A.E. Berkowitz, Appl. Phys. Lett. 64 (1994) 3652.
[9] F.E. Luborsky, J.J. Becker, R.O. Cary, IEEE Trans. Magn. Mag-11 (1975) 1644.
[10] J. González, K. Kulakowski, J. Magn. Magn. Mater. 82 (1989) 94.
[11] C. García, A. Chizhik, J.J. del Val, A. Zhukov, J.M. Blanco, J. González, J. Magn. Magn. Mater. 294 (2005) 193.
[12] M. Vázquez, J. González, A. Hernando, J. Magn. Magn. Mater. 53 (323) (1986).
[13] V. Zhukova, A.F. Cobeño, A. Zhukov, J.M. Blanco, S. Puerta, J. Gonzalez, M. Vázquez, J. Non-crystalline Solids 287 (2001) 31–36.
[14] J.M. Barandiaran, L.F. Barquin, J.C.G. Sal, P. Gorria, A. Hernando, Solid State Commun. 88 (1) (1993) 75–80.
[15] J. González, J.M. Blanco, M. Vázquez, J.M. Barandiarán, G. Rivero, A. Hernando, J. Appl. Phys. 70 (1991) 6522.
[16] P. Aragoneses, J.M. Blanco, L. Dominguez, J. González, A. Zhukov, M. Vázquez, J. Phys. D: Appl. Phys. 31 (1998) 3040–3045.